

(44)  $[M^+ - \text{thf} - \text{C}_6\text{Cl}_4\text{O}_2]$ , 446 (100)  $[MH^+ - \text{thf} - \text{C}_6\text{Cl}_4\text{O}_2 - \text{C}_7\text{H}_{12}]$ ; elemental analysis calcd for  $\text{C}_{30}\text{H}_{28}\text{Cl}_8\text{O}_3\text{Pd}$  (858.58): C 41.97, H 3.29; found: C 42.27, H 3.43.

**5:** The diethyl ether complex **4a** (86.1 mg, 0.10 mmol) was dissolved in dry degassed pyridine (1 mL) and stirred at room temperature for 30 min. The solution was filtered through a glass frit and the filtrate was diluted with dry degassed pentane (30 mL) before being cooled overnight at about  $-15^\circ\text{C}$ . The obtained brown crystals were collected on a glass frit and dried under vacuum at room temperature for 48 h. The yield was 76.7 mg (75.6%): m.p. 99.2–99.5  $^\circ\text{C}$  (decomp);  $^1\text{H}$  NMR (300 MHz,  $\text{CDCl}_3$ ):  $\delta$  = 1.16–1.32 (m, 1H), 1.34–1.46 (m, 1H), 1.54–1.80 (m, 3H), 2.71 (d,  $J$  = 3.8 Hz, 1H), 2.75 (d,  $J$  = 3.8 Hz, 1H), 3.00 (d,  $J$  = 10.2 Hz, 1H), 4.03 (s, 2H), 7.25 (dd,  $J$  = 7.8, 4.2 Hz, 4H), 7.67 (tt,  $J$  = 7.8, 1.5 Hz, 1H), 8.51 ppm (d,  $J$  = 4.2 Hz, 4H); MS (FAB)  $m/z$  (%) 541 (34)  $[M^+ - 3\text{Py} - \text{C}_6\text{Cl}_4\text{O}_2]$ , 446 (100)  $[MH^+ - 3\text{Py} - \text{C}_6\text{Cl}_4\text{O}_2 - \text{C}_7\text{H}_{12}]$ ; elemental analysis calcd (%) for  $\text{C}_{41}\text{H}_{35}\text{Cl}_8\text{N}_3\text{O}_3\text{Pd}$  (1023.78): C 48.10, H 3.45, N 4.10; found: C 47.93, H 3.41, N 3.91.

Received: June 6, 2002 [Z19483]

- [1] J. Tsuji, *Palladium Reagents and Catalysts*, Wiley, Chichester, **1995**.
- [2] a) M. Catellani, M. C. Fagnola, *Angew. Chem.* **1994**, *106*, 2559–2561; *Angew. Chem. Int. Ed. Engl.* **1994**, *33*, 2421–2422; b) M. Catellani, F. Frignani, A. Rangoni, *Angew. Chem.* **1997**, *109*, 142–145; *Angew. Chem. Int. Ed. Engl.* **1997**, *36*, 119–122; c) M. Catellani, F. Cugini, *Tetrahedron* **1999**, *55*, 6595–6602; d) M. Catellani, E. Motti, M. Minari, *Chem. Commun.* **2000**, 157–158; e) M. Catellani, E. Motti, S. Baratta, *Org. Lett.* **2001**, *3*, 3611–3614.
- [3] a) D. Milstein, J. K. Stille, *J. Am. Chem. Soc.* **1979**, *101*, 4981–4991; b) D. Milstein, J. K. Stille, *J. Am. Chem. Soc.* **1979**, *101*, 4992–4998; c) I. Guibert, D. Neibecker, I. Tkatchenko, *J. Chem. Soc. Chem. Commun.* **1989**, 1850–1852; d) B. M. Trost, *Acc. Chem. Res.* **1990**, *23*, 34–42; e) T. Yoneyama, R. H. Crabtree, *J. Mol. Catal. A* **1996**, *108*, 35–40; f) R. van Belzen, H. Hoffmann, C. J. Elsevier, *Angew. Chem.* **1997**, *109*, 1833–1835; *Angew. Chem. Int. Ed. Engl.* **1997**, *36*, 1743–1745; g) R. van Belzen, R. A. Klein, H. Kooijman, N. Veldman, A. L. Spek, C. J. Elsevier, *Organometallics* **1998**, *17*, 1812–1825; h) B. L. Shaw, *New J. Chem.* **1998**, 77–79.
- [4] a) G. K. Anderson in *Comprehensive Organometallic Chemistry II*, Vol. 9 (Eds.: R. J. Puddephatt, E. W. Abel, F. G. A. Stone, G. Wilkinson), Pergamon, Oxford, **1995**, chap. 8, pp. 497–507; b) L. M. Rendina, R. J. Puddephatt, *Chem. Rev.* **1997**, *97*, 1735–1754.
- [5] P. K. Byers, A. J. Canty, B. W. Skelton, A. H. White, *J. Chem. Soc. Chem. Commun.* **1986**, 1722–1724.
- [6] a) A. J. Canty, *Acc. Chem. Res.* **1992**, *25*, 83–90; b) A. J. Canty in *Comprehensive Organometallic Chemistry II*, Vol. 9 (Eds.: R. J. Puddephatt, E. W. Abel, F. G. A. Stone, G. Wilkinson), Pergamon, Oxford, **1995**, chap. 5, pp. 272–276; c) A. J. Canty, G. van Koten, *Acc. Chem. Res.* **1995**, *28*, 406–413; d) A. J. Canty, J. Patel, M. Pfeffer, B. W. Skelton, A. H. White, *Inorg. Chim. Acta* **2002**, *327*, 20–25, and references therein.
- [7] R. A. Klein, P. Witte, R. van Belzen, J. Fraanje, K. Goubitz, M. Numan, H. Schenk, J. M. Ernsting, C. J. Elsevier, *Eur. J. Inorg. Chem.* **1998**, 319–330, and references therein.
- [8] a) C. G. Pierpont, R. M. Buchanan, *Coord. Chem. Rev.* **1981**, *38*, 45–87; b) C. G. Pierpont, *Coord. Chem. Rev.* **2001**, *219–221*, 415–433.
- [9] A. L. Balch, *J. Am. Chem. Soc.* **1973**, *95*, 2723–2724.
- [10] Crystallographic data: Intensity data were collected at 173 K on a Bruker SMART APEX diffractometer with  $\text{MoK}_\alpha$  radiation (0.71073 Å) and graphite monochromator. The absorption correction was made using SADABS. The structure was solved by direct methods and refined by the full-matrix least-squares on  $F^2$  (SHELXTL). **4b**:  $\text{C}_{30}\text{H}_{28}\text{Cl}_8\text{O}_3\text{Pd}$ ,  $M_r$  = 858.58, space group  $P2(1)/n$  (no. 14), monoclinic,  $a$  = 10.0282(7),  $b$  = 21.2453(15),  $c$  = 15.1970(11) Å,  $\beta$  = 90.171(2)°,  $V$  = 3237.7(4) Å<sup>3</sup>;  $Z$  = 4,  $\rho_{\text{calcd}}$  = 1.761 g cm<sup>-3</sup>; a total of 24938 reflections were measured and 8652 were independent [ $R(\text{int})$  = 0.0245]. Final  $R_1$  = 0.0275,  $wR_2$  = 0.0725 [ $I > 2\sigma(I)$ ], and GOF = 0.743 (for all data,  $R_1$  = 0.0329,  $wR_2$  = 0.0778). **5**:  $\text{C}_{41}\text{H}_{35}\text{Cl}_8\text{N}_3\text{O}_3\text{Pd}$ ,  $M_r$  = 1023.78; space group  $P\bar{1}$  (no. 2), triclinic,  $a$  = 10.4110(5),  $b$  = 12.2527(6),  $c$  = 18.4200(9) Å,  $\alpha$  = 75.0470(10),  $\beta$  = 75.0760(10),  $\gamma$  = 66.4740(10)°,  $V$  = 2049.57(17) Å<sup>3</sup>;  $Z$  = 2,  $\rho_{\text{calcd}}$  = 1.659 g cm<sup>-3</sup>; a total of 16045 reflections were measured and 10743 were independent [ $R(\text{int})$  = 0.0203]. Final

$R_1$  = 0.0302,  $wR_2$  = 0.0811 [ $I > 2\sigma(I)$ ], and GOF = 0.733 (for all data,  $R_1$  = 0.0320,  $wR_2$  = 0.0832). CCDC-186953 (**4b**) and CCDC-186954 (**5**) contains the supplementary crystallographic data for this paper. These data can be obtained free of charge via [www.ccdc.cam.ac.uk/conts/retrieving.html](http://www.ccdc.cam.ac.uk/conts/retrieving.html) (or from the Cambridge Crystallographic Data Centre, 12, Union Road, Cambridge CB21EZ, UK; fax: (+44) 1223-336-033; or deposit@ccdc.cam.ac.uk).

- [11] C. G. Pierpont, H. H. Downs, *Inorg. Chem.* **1975**, *14*, 343–347.
- [12] M. B. Smith, M. J. March, *March's Advanced Organic Chemistry*, Part 1, 5th ed., Wiley, New York, **2001**, chap. 1, p. 20.
- [13] a) A. J. Canty, H. Jin, *J. Organomet. Chem.* **1998**, *565*, 125–140; b) A. J. Canty, H. Jin, B. W. Skelton, A. H. White, *Inorg. Chem.* **1998**, *37*, 3975–3981; c) A. J. Canty, M. C. Done, B. W. Skelton, A. H. White, *Inorg. Chem. Commun.* **2001**, *4*, 648–650.
- [14] R. Noyori, *Asymmetric Catalysis in Organic Synthesis*, Wiley, New York, **1994**.

## Direct Assembly of Large Arrays of Oriented Conducting Polymer Nanowires\*\*

Liang Liang, Jun Liu,\* Charles F. Windisch, Jr., Gregory J. Exarhos, and Yuehe Lin

Recently, oriented carbon nanotubes, and nanowires of semiconductors, oxides, and metals have attracted wide attention. However, there have been few reports on the direct growth of oriented polymer nanostructures such as oriented polymer nanowires. Oriented conducting polymer nanostructures will be very useful for many applications,<sup>[1–3]</sup> which range from chemical and biological sensing and diagnosis to energy conversion and storage (photovoltaic cells, batteries and capacitors, and hydrogen-storage devices), light-emitting display devices, catalysis, drug delivery, separation, microelectronics, and optical storage.

Several methods, which include electrospinning<sup>[4,5]</sup> and polymer-templated electrochemical synthesis,<sup>[6]</sup> have been used for preparing conducting polymer nanofibers. Highly porous, conducting polymer films based on techniques such as dip coating on porous supports have been widely investigated for separation and sensing,<sup>[7]</sup> but the random pore structures and misalignment of the polymers are not ideal for high efficiency and faster kinetics. Controlled orientation is more critical for applications such as in light-emitting and micro-

[\*] Dr. J. Liu  
Sandia National Laboratories  
Biomolecular Materials and Interfaces Department  
P.O. Box 5800, Mail Stop 1413, Albuquerque NM 87185-1413 (USA)  
Fax: (+1) 505-844-5470  
E-mail: jliu@sandia.gov  
C. F. Windisch, Jr., G. J. Exarhos, Y. Lin  
Pacific Northwest National Laboratory  
902 Battelle Boulevard, P.O. Box 999, Richland, WA 99352 (USA)  
L. Liang  
Now at: eVionyx, 6 Skyline Drive, Hawthorne, NY10532 (USA)

[\*\*] This research was supported by the Office of Basic Energy Sciences, Materials Division, of the Department of Energy at the Pacific Northwest National Laboratory, Richland, Washington. We would like to thank Dr. Zhengrong Tian from Sandia National Laboratories for his helpful discussions of the manuscript.

electronic devices. To date, oriented conducting polymer nanostructures, including oriented polypyrrole or polyaniline nanorods or nanotubes, were mostly obtained with a porous membrane as the template.<sup>[8–13]</sup> Recently, Gao et al.<sup>[14]</sup> used oriented carbon nanotubes as the template to deposit a thin polyaniline-polymer coating on the surface of the carbon nanotubes electrochemically. In the templated approach, the dimensions and the morphology of the polymer structures are defined (or limited) by the porous support. The formation of arrays of oriented polymer rods or tubes involves carefully etching away the membrane without disturbing the conducting polymer structure. Published results indicate that oriented structures were only obtained for rods and tubes with a large diameter.<sup>[15]</sup> Etching away the membrane supports for nanorods or tubes with a diameter smaller than 100 nm caused the polymer to collapse into structures without preferred orientation.<sup>[15]</sup>

Herein, we report the direct electrochemical synthesis of large arrays of uniform and oriented nanowires of conducting polymers with a diameter much smaller than 100 nm, on a variety of substrates (Pt, Si, Au, carbon, silica), without using a supporting template. Compared with membrane-templated synthesis, it is easier to prepare oriented conducting polymer nanostructures on complicated surfaces (such as on a micro-electrode surface) through direct electrochemical deposition, therefore opening up new opportunities for designing devices. We first observed that if polyaniline were deposited under a galvanostatic current density of  $0.08 \text{ mA cm}^{-2}$ , a value higher than that reported in the literature ( $0.017 \text{ mA cm}^{-2}$ , for example),<sup>[16]</sup> polyaniline nanoparticles, rather than continuous films, were observed on the substrate under our experimental conditions. We hypothesized that we could use these polyaniline particles as the nucleation sites to grow extended polymer nanostructures by adding a second or a third deposition step with a reduced current density. Therefore, we designed a three-step electrochemical deposition procedure. In the first step, a large current density was used to create the nucleation sites on the substrate. The initial stage was followed by continued polymerization with reduced current density. A typical procedure involves electrochemical deposition in an aniline-containing electrolyte solution, by using the substrate as the working electrode. This process involves:  $0.08 \text{ mA cm}^{-2}$  for 0.5 h, followed by  $0.04 \text{ mA cm}^{-2}$  for 3 h, which was then followed by another 3 h at  $0.02 \text{ mA cm}^{-2}$ . The stepwise growth produced uniform, oriented nanowires on a variety of flat and rough surfaces. The amount of aniline polymerized is estimated to be  $1.1 \times 10^{-3} \text{ mmol monomer cm}^{-2}$  ( $0.1 \text{ mg aniline cm}^{-2}$ ) for the first step,  $4.5 \times 10^{-3} \text{ mmol monomer cm}^{-2}$  (or  $0.42 \text{ mg cm}^{-2}$ ) for the second step, and  $2.2 \times 10^{-3} \text{ mmol monomer cm}^{-2}$  (or  $0.21 \text{ mg cm}^{-2}$ ) for the third step, respectively.

The polyaniline films prepared by the above method appear to be fairly uniform by visual inspection. The color is intensely black and nonreflective. The morphology of the film was examined under a field emission-scanning electron microscope (SEM). When viewed from an angle perpendicular to the surface at a low magnification (Figure 1a), the film appears to contain uniform white dots all across the surface. At a higher magnification (Figure 1b), it is revealed that the

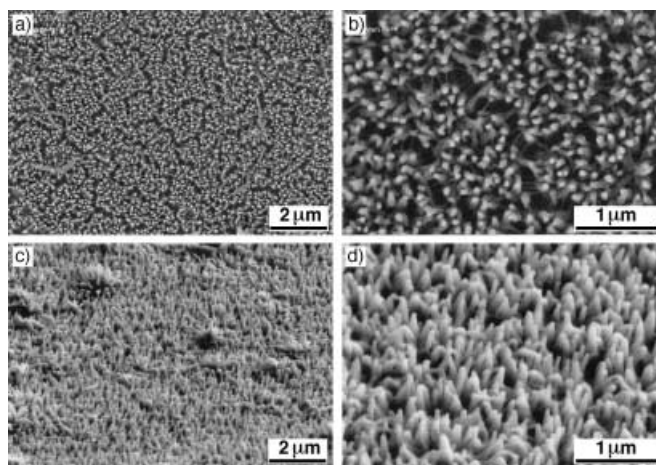


Figure 1. SEM micrographs of oriented polyaniline on Pt: a) low magnification face-on; b) high magnification face-on; c) tilted view, low magnification; d) tilted view, high magnification.

white dots are actually the tips of uniform nanowires, mostly oriented perpendicular to the substrate. The diameters of the tips range from 50 nm to 70 nm. There are also some thin filament structures, approximately 20 nm in diameter, at the base of the oriented nanowires. When the sample is tilted, the morphology and the orientation of the nanowires are clearly revealed (Figure 1c and d). The oriented nanowires are fairly uniform in length and diameter, but the diameter is slightly smaller at the tip position than at the base position. From the tilt angle (about  $40^\circ$ ), the nanowires are estimated to be  $0.8 \mu\text{m}$  in length.

To investigate how the oriented nanowires were formed, we examined a sample after the first step ( $0.08 \text{ mA cm}^{-2}$  for 0.5 h) (Figure 2a). At this stage the polymer was deposited on the

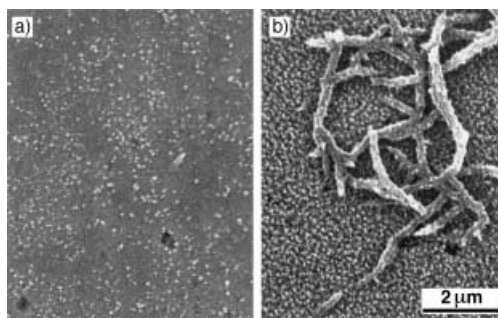


Figure 2. Growth stages of polyaniline on Pt: a) polyaniline particles after 0.5 h at  $0.08 \text{ mA cm}^{-2}$ ; b) polyaniline particles and fibers after 3 h at  $0.08 \text{ mA cm}^{-2}$ .

surface as small particles about 50 nm in diameter. If the electrochemical deposition was extended for several hours under the same current density ( $0.08 \text{ mA cm}^{-2}$ ), a much higher density of polymer was deposited (Figure 2b), but long, oriented nanowires were not observed. In addition, thick-branched polymer fibers of hundreds of nm in diameter began to form at many locations. Only when the current density was successively reduced were uniform and oriented nanowires formed (Figure 1). We suggest that the nanowires are formed by the following mechanisms (Figure 3a): 1) nucleation on the

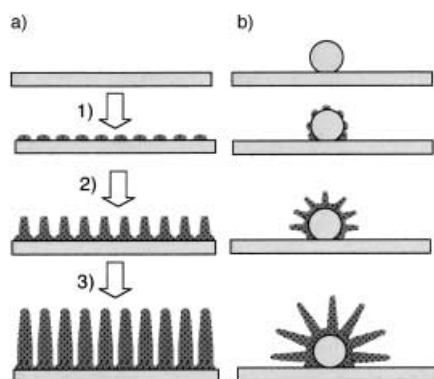


Figure 3. Schematic illustration of the nucleation and growth of polyaniline nanowires, a) on a flat substrate, and b) on a colloidal particle.

substrate at a high current density, and 2) continued nucleation and growth at the low current density.

Understanding how the oriented nanowires are formed suggests useful approaches to control the orientation of the polymers. We first deposited a monolayer of closely packed silica spheres on the substrate and expected that the polymer nanowires would grow with an orientation perpendicular to the particle surfaces (not to the substrate surface; Figure 3b). To illustrate how the polymer grows from the silica particles, we show the results in an area where the particles were not closely packed. Figure 4a shows the surface roughness induced by the presence of silica particles, which follow the contours of the individual particles. The radial growth of the polymer wires around the particles is clearly illustrated. Figure 4b shows the morphology of the polymers across the edge of the silica monolayer. Close to the edge where there are no silica particles, the polymers are oriented vertically, but on top of the silica particles the polymer orientation is disrupted and randomly connected. In the area occupied by a monolayer of densely packed silica spheres, the radial growth of polymer nanowires overlap and form 3D-interconnected polymer networks (Figure 4c and 4d). Such morphologies

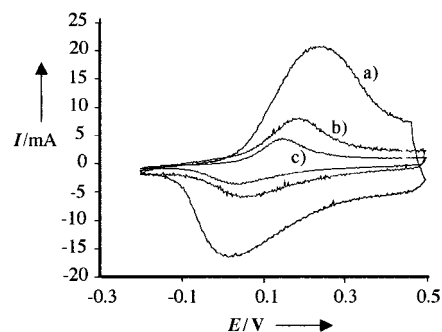


Figure 5. Cyclic voltammograms of different polyaniline morphologies: a) oriented polymer nanowires on Pt; b) interconnected polymer fibers on Pt with silica spheres; c) polymer deposited without stepwise control of the current density.

oriented nanowires (see Figure 1), samples deposited at constant current density (see Figure 2b), and interconnected nanofibers deposited with colloidal silica (see Figure 4). All samples demonstrated electrochemical activity, which is characterized by the typical reduction and oxidation responses.<sup>[17,18]</sup> However, the oriented nanowires have considerably higher redox current than the interconnected nanofibers, which in turn have a higher redox current than the samples prepared with a constant current. The difference in the redox currents reflects the effective active surface areas that are accessible to the electrolytes. Apparently, the oriented nanowires have the highest effective surface area, which is desirable for high efficiency and sensitivity of many devices.

In summary, we were able to deposit directly large arrays of oriented conducting polymer nanowires on a variety of substrates without a porous membrane support. This is a very novel approach for synthesizing oriented polymer nanostructures and we believe that it will have great potential for microsensors and other microelectronic and optical devices.

#### Experimental Section

**Oriented nanowires on Pt and other substrates:** A Pt plate was washed thoroughly with ethanol and dried in air. The Pt foil was further rinsed in a 1 wt.% sodium dodecyl sulfate (SDS) solution to improve the wetting behavior with water and dried in air. Electrochemical deposition of polyaniline was performed by immersing the Pt plate into the aqueous solution containing 0.5M aniline and 1.0M perchloric acid ( $\text{HClO}_4$ ). The effective area of the immersed Pt plate is 4.5 cm<sup>2</sup>. Polyaniline was grown from the surface of the platinum plate by redox polymerization using an EG&G Princeton Applied Research Model 273 potentiostat/galvanostat controlled by a personal computer with EG&G Princeton Applied Research Model 270 electrochemical software. A one-compartment cell was used with another platinum plate as the counter electrode. The same instrument was used for the voltammetry measurements. Besides Pt, other substrates, including Ti, Au, Si, were investigated and yielded similar results.

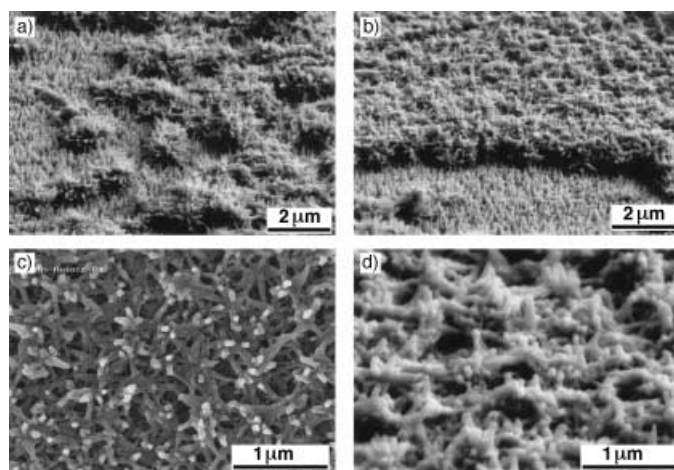


Figure 4. Interconnected conducting nanofibers with colloidal silica. a) Radial growth of the nanowires from single silica particles; b) the morphology of nanofibers on the edge of the colloidal silica monolayer; c) top view of the interconnected nanofibers; d) tilted view of the oriented nanofibers.

Preparation of polyaniline with a monolayer of colloidal silica: To control the morphology of the polymer, a monolayer of close packed colloidal silica (0.5  $\mu\text{m}$  diameter standard silica spheres obtained from Duke Scientific, Palo Alto, California) was first deposited on the Pt substrate. After the Pt plate was rinsed with the SDS solution, a droplet of a colloidal silica solution containing 0.4 wt. % silica particles was placed on the Pt substrate. The SDS treatment improved the wetting behavior of the silica colloidal solution and allowed the droplet to spread over the whole surface of the Pt plate. The excess solution was removed from the substrate by positioning the Pt plate vertically to allow the excess water to flow off. After drying, the Pt plate with the silica particles was heated in an oven at 110°C for 0.5 h. Electrochemical deposition of polyaniline was conducted using the same procedure.

Received: March 1, 2002  
Revised: May 13, 2002 [Z18806]

- [1] A. G. MacDiarmid, *Rev. Mod. Phys.* **2001**, 73, 701.
- [2] K. Dobhofer, K. Rajeshwar, *Handbook of Conducting Polymers*, Marcel Dekker, New York, **1998**, chap. 20.
- [3] D. Kumar, R. C. Sharma, *Eur. Polym. J.* **1998**, 34, 1053.
- [4] J. Doshi, D. H. Reneker, *J. Electrostat.* **1999**, 35, 151.
- [5] D. H. Renek, A. L. Yarin, H. Fong, S. Koombhongse, *J. Appl. Phys.* **2000**, 87, 4531.
- [6] C. Jérôme, R. Jérôme, *Angew. Chem.* **1998**, 110, 2639; *Angew. Chem. Int. Ed.* **1998**, 37, 2488.
- [7] H. S. Lee, J. Hong, *Synth. Met.* **2000**, 113, 115.
- [8] A. Huczko, *Appl. Phys. A* **2000**, 70, 365.
- [9] C. R. Martin, *Chem. Mater.* **1996**, 8, 1739.
- [10] M. Nishizawa, K. Mukai, S. Kuwabata, C. R. Martin, H. Yoneyama, *J. Electrochem. Soc.* **1997**, 144, 1923.
- [11] S. De Vito, C. R. Martin, *Chem. Mater.* **1998**, 10, 1738.
- [12] S. M. Marienakos, L. C. Brousseau III, A. Jones, D. L. Feldheim, *Chem. Mater.* **1998**, 10, 1214.
- [13] C.-G. Wu, T. Bein, *Science* **1994**, 264, 1757.
- [14] M. Gao, S. Huang, L. Dai, G. Wallace, R. Gao, Z. Wang, *Angew. Chem.* **2000**, 112, 3810; *Angew. Chem. Int. Ed.* **2000**, 39, 3664.
- [15] J. Duchet, R. Legras, S. Demoustier-Champagne, *Synth. Met.* **1998**, 98, 113.
- [16] A. A. Nekrasov, V. F. Ivanov, O. L. Grikova, A. V. Vannikov, *J. Electroanal. Chem.* **1996**, 412, 133.
- [17] B. Y. Choi, I. J. Chung, J. H. Chun, J. M. Ko, *Synth. Met.* **1999**, 99, 253.
- [18] S. B. Adeloju, G. G. Wallace, *Analyst* **1996**, 121, 699.

## A New Generation of Air Stable, Highly Active Pd Complexes for C–C and C–N Coupling Reactions with Aryl Chlorides\*\*

Anita Schnyder, Adriano F. Indolese,\*  
Martin Studer,\* and Hans-Ulrich Blaser

Palladium-catalyzed coupling reactions such as the Suzuki coupling, the Heck reaction, and the Buchwald–Hartwig amination or arylation of ketones are now standard transformations in both academic and industrial laboratories.<sup>[1]</sup> While simple palladium salts are excellent catalysts for reactive substrates, such as aryl iodides, activated aryl bromides, or aromatic diazo compounds, the less reactive but commercially very interesting aryl chlorides require palladium catalysts activated and stabilized by additional ligands. A crucial factor for a successful catalyst is the choice of the right ligand, most frequently an electron-rich, bulky tertiary phosphane, and in recent years a number of very effective ligands have been developed for the reactions mentioned above.<sup>[2]</sup>

However, these customized phosphanes are usually expensive and their synthesis can be difficult, often involving multistep syntheses using air-sensitive substances. An interesting alternative could be secondary phosphanes, many of which are available in bulk quantities at a relatively low price. Even though their application in transition-metal catalysis is rare,<sup>[3]</sup> we recently found that secondary dialkyl phosphanes such as HP(*tert*-butyl)<sub>2</sub> and HP(adamantyl)<sub>2</sub> can indeed be applied successfully for the palladium-catalyzed Heck reaction even with notoriously unreactive, electron-rich aryl chlorides.<sup>[4]</sup>

This result encouraged us to investigate other palladium-catalyzed reactions (Scheme 1) using a combinations of palladacycles and secondary phosphanes. Palladacycles have recently been described as versatile catalyst precursors for a number of coupling reactions<sup>[5]</sup> and they can be regarded as stable, easily accessible aryl palladium species. Catalyst libraries with high diversity could readily be prepared with this strategy since a wide variety of palladacycles and secondary phosphanes are available.

[\*] Dr. A. F. Indolese  
Rohner AG, Gempenstrasse 6  
4133 Pratteln (Switzerland)  
Fax: (+41) 61-825-3112  
E-mail: aindolese@rohnerag.ch  
Dr. M. Studer, Dr. A. Schnyder, Dr. H.-U. Blaser  
Solvias AG, WRO 1055.6  
P.O. Box, 4002 Basel (Switzerland)  
Fax: (+41) 61-686-6311  
E-mail: martin.studer@solvias.com

[\*\*] This work was supported by the Novartis Forschungsstiftung. We thank M. Beller (IfOK, Rostock) F. Naud, and M. Pugin (Solvias) for stimulating discussions, T. Aemmer, L. Troendlin, and A. Marti for careful experimental work, and M. Pfeffer (CNRS Strassbourg) for helpful suggestions regarding the preparation of the palladacycles. The secondary phosphanes were generously provided by Cytec Industries, Niagara Falls (A. Roberston, O. Rouher).



Supporting information for this article is available on the WWW under <http://www.angewandte.org> or from the author.